



HAL
open science

Design and performance evaluation of air core inductors for Very High Frequency power conversion

Florentin Salomez, Vincent Blanchon, Sébastien Carcouet, J-L. Schanen, G.
Despesse, Yves Lembeye

► To cite this version:

Florentin Salomez, Vincent Blanchon, Sébastien Carcouet, J-L. Schanen, G. Despesse, et al.. Design and performance evaluation of air core inductors for Very High Frequency power conversion. PCIM Europe 2024 - International Exhibition and Conference for Power Electronics, Intelligent Motion, Renewable Energy and Energy Management, Jun 2024, Nuremberg, Germany. 10.30420/566262341 . hal-04720848

HAL Id: hal-04720848

<https://hal.science/hal-04720848v1>

Submitted on 4 Oct 2024






HAL is a multi-disciplinary open access archive for the deposit and dissemination of scientific research documents, whether they are published or not. The documents may come from teaching and research institutions in France or abroad, or from public or private research centers.

L'archive ouverte pluridisciplinaire **HAL**, est destinée au dépôt et à la diffusion de documents scientifiques de niveau recherche, publiés ou non, émanant des établissements d'enseignement et de recherche français ou étrangers, des laboratoires publics ou privés.



Distributed under a Creative Commons Attribution - NonCommercial - ShareAlike 4.0 International License

Design and Performance Evaluation of Air Core Inductors for Very High Frequency Power Conversion

Florentin Salomez ¹, Vincent Blanchon ², Sébastien Carcouet², Jean-Luc Schanen ¹, Ghislain Despesse ², Yves Lembeye ¹

¹ Univ. Grenoble Alpes, CNRS, Grenoble INP, G2ELAB, 38000 Grenoble, France

² CEA-Leti, Univ. Grenoble Alpes, F-38000 Grenoble, France

Corresponding author: Florentin Salomez, florentin.salomez@grenoble-inp.fr

Speaker: Florentin Salomez, florentin.salomez@grenoble-inp.fr

Abstract

This paper shows a simple performance evaluation of rectangular cross section air core solenoids based on analytical approach validated on prototypes. The asymptotic behaviors of the quality factor as a function of geometrical parameters show the theoretical range of inductance and resistance of solenoids made out of planar substrate like Printed Circuit Board.

1 Introduction

The renewed interest in VHF converters [1] comes in part from the need to miniaturized the low power switch-mode power supply without sacrificing the efficiency [2], [3], and to improve wireless power transfer [4], [5]. The goal of this paper is to present a way to increase the mass power density of very high frequency (VHF) converters thanks to air core inductors without sacrificing the efficiency. In the literature one of the most used technology is the inductor integrated in the Printed Circuit Board (PCB) [6]–[10]. Numerical optimization is used to find the inductor with the best Q factor in [6], [7], [10], sometimes in conjunction with Finite Element software for solenoids [6], [8] and for ring cores [9]. None of the papers cited before has quantify the theoretical limit of Q factor one can achieve with PCB inductor technology. This paper addresses the theoretical limits of the Q factor of a rectangular cross-section solenoid for a given substrate thickness and area, which is very important to assess the potential of the air core technology for VHF power conversion with functionalised PCB [6], [7], [9], [10]. First the model of the Q factor of air core solenoids with a rectangular cross section is derived. Second, this model is used to study the theoretical limit of the Q factor and experiments are performed to validate the results. Third, experimental results of air core solenoids inside a VHF converter are presented.

Finally, some conclusions and perspectives are presented.

2 Modelling of the Solenoid

2.1 Geometrical Description

A solenoid with a rectangular cross-section and made with copper tape is considered hereafter and drawn in the Figure 1, with t the thickness of the substrate, w_t the width of the trace, w_{ti} the width of the trace at the edge, s_t the interturn space, θ the angle between the traces and the cross-section, w the width of the solenoid, l its length, $S_{top} = l \cdot w$ its footprint area, $k = l/w$ its form factor and N the number of turns. Some of the preceding variables

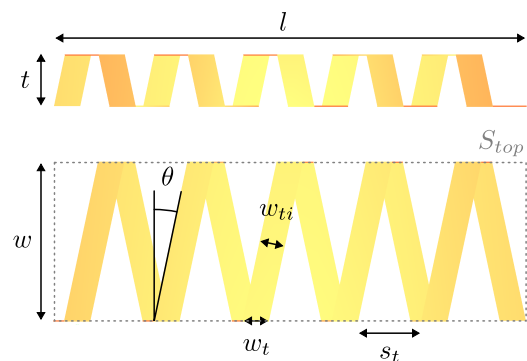


Fig. 1: Drawing of the rectangular cross-section solenoid with exaggerated inter-turns space s_t .

are linked by the following equations:

$$w_{ti} = \frac{w_t}{\cos(\theta)}, \quad (1)$$

$$l = N \cdot (w_{ti} + s_t) + w_{ti}, \quad (2)$$

$$w_{ti} + s_t = 2 \cdot (h + w) \cdot \tan(\theta). \quad (3)$$

It is possible to express θ as a function of input parameters N, l, s_t such that

$$\theta = \arctan\left(\frac{\frac{l-s_t}{N+1} + s_t}{2\pi r}\right). \quad (4)$$

2.2 Inductance, Resistance and Q Factor

The parasitic capacitance of the solenoid is neglected. Its inductance is defined by

$$L = \mu_0 N^2 \frac{tw}{l} = \mu_0 N^2 \frac{t}{k}, \quad (5)$$

with μ_0 the permeability of the vacuum. The direct current (DC) resistance of the component is

$$R_{DC} = \rho \cdot \frac{2 \cdot N \cdot (t + w)}{t_{Cu} \cdot w_t \cdot \cos(\theta)}, \quad (6)$$

with ρ the copper resistivity and t_{Cu} its thickness. The alternating current (AC) resistance is approximated as the resistance of the skin depth $\delta(f)$ along the conductor (if the thickness of the conductor is greater than the skin depth at the considered frequency, proximity effects are neglected) and defined by

$$R_{AC} = \frac{t_{Cu}}{\delta(f)} R_{DC}. \quad (7)$$

The Q factor is defined as

$$Q = \frac{2\pi f L}{R_{AC}}. \quad (8)$$

3 Performance Evaluation

The evaluation of performance consists of studying the variation of the Q factor as a function of the geometrical parameters of the solenoids to assess the potential of the technology. The Q factor is frequency dependent. Since the ultimate goal of the paper is to design an inductance for a VHF converter, all computations and results are presented at the frequency 27.12 MHz of the second harmonic of the converter which is filtered by a parallel LC branch.

3.1 Asymptotic Behaviors

Assuming θ is small leads to $w_t \approx w_{ti}$ and $\cos(\theta) \approx 1$ and substituting w_{ti} thanks to Equation (2) leads to the approximation $Q \approx Q_a$ with

$$Q_a = \frac{\pi f \mu_0 \cdot \delta(f)}{\rho} \cdot \frac{N}{N+1} \cdot \frac{tw}{t+w} \cdot \frac{l - N \cdot s_t}{l}. \quad (9)$$

It is also possible to rewrite the previous equation with k and S_{top} such that

$$Q_a = \frac{\pi f \mu_0 \delta(f)}{\rho} \cdot \frac{N}{N+1} \cdot \frac{t}{t \cdot \sqrt{\frac{k}{S_{top}} + 1}} \cdot \left(1 - \frac{N \cdot s_t}{\sqrt{k \cdot S_{top}}}\right) \quad (10)$$

The theoretical maximum Q factor for a given PCB thickness Q_{max} is defined thanks to the following assumptions: the number of turns is large enough such that

$$\frac{N}{N+1} \underset{N \gg 1}{\approx} 1, \quad (11)$$

the width w is greater than the substrate thickness t such that

$$\beta = \frac{tw}{t+w} \underset{w \gg t}{\approx} t, \quad (12)$$

the inter-tuns space s_t is small enough in comparison to l such that

$$\frac{l - N \cdot s_t}{l} \underset{N \cdot s_t \ll l}{\approx} 1, \quad (13)$$

and the skin depth is

$$\delta(f) = \sqrt{\frac{\rho}{\pi f \mu_0}}. \quad (14)$$

These asymptotic behaviors ($N \gg 1$, $w \gg t$, $N \cdot s_t \ll l$) lead to

$$Q_a \sim Q_{max} = \frac{t}{\delta(f)} = \sqrt{\frac{\pi f \mu_0}{\rho}} \cdot t, \quad (15)$$

meaning that **the thickness of the PCB t is the main parameter to increase the Q factor**. This is experimentally verified in the Figure 2 where two solenoids of same parameters apart thickness have been characterized. The solenoids are depicted in the Figure 3 and the details about their dimensions and electrical performances are given in the Table 1. An impedance analyzer *E4990A* equipped with the adapter *42942A* and the socket *16092A* has been used for Q measurement. The adapter has been calibrated with open, short, load and low loss standards and the socket has been compensated for open and short parasitic impedances to ensure the accuracy of the measurement of Q factor.

Tab. 1: Dimensions and electrical characteristics of the tested solenoids at $f = 27.12$ MHz.

ld.	t (mm)	w (mm)	l (mm)	N	L (nH)	R (m Ω)	Q
A1	2	17	17	6	104	187	95
A2	2	21	21	6	113	214	89
A3	2	24	24	6	109	173	107
B1	2	24	22	4	58	93	107
B2	2	24	24	9	231	428	92
T5	5	24	24	6	222	224	168

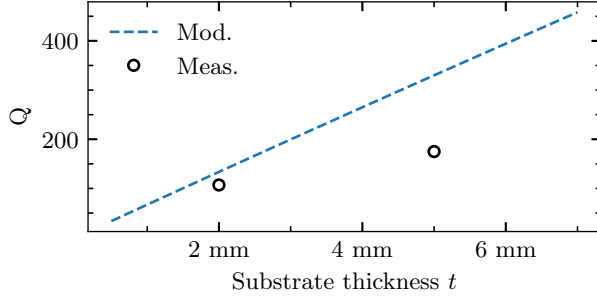


Fig. 2: Evolution of Q for two different substrate thickness t at $f = 27.12$ MHz.



Fig. 3: Photograph of the solenoids characterised in the Figure 2, with ($l = w = 2.4$ mm, $s_t = 0.5$ mm, $N = 6$).

3.2 Evolution of Q as a Function of Footprint Area S_{top}

According to Equation (5) the inductance is only a function of the number of turns, the thickness and the form factor. Since L is independent of S_{top} , it is possible to study the evolution of Q as a function of S_{top} for a given inductance L . The Equation (10) shows that Q_a is increasing monotonically for an increasing footprint surface S_{top} . The theoretical evolution is plotted in the Figure 4 alongside three measurement points (A1, A2, and A3). The photographs of the characterized solenoids A1, A2, and A3 are presented in the Figure 5. The Figure 4 shows the asymptotic behavior of Q which reaches

$$\frac{N}{N+1} \cdot Q_{max}, \quad (16)$$

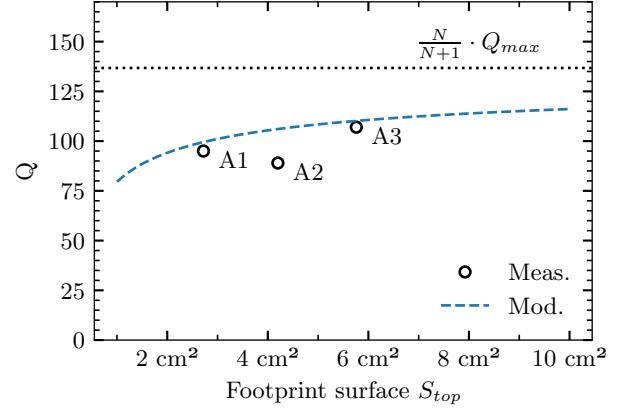


Fig. 4: Evolution of Q as a function of S_{top} for given frequency f , s_t , L and t .

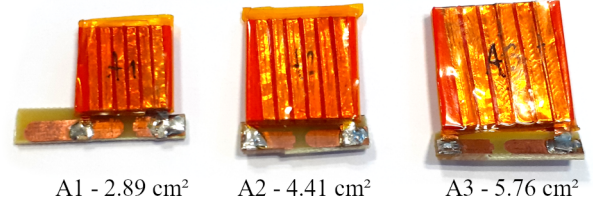


Fig. 5: Photograph of the solenoids A1, A2 and A3 characterized in Figure 4.

as S_{top} tends to $+\infty$. **The Q factor tends to a limit as S_{top} increases. This asymptotic behavior shows that increasing Q factor once the thickness has been fixed is possible but at the expense of a large footprint area.**

3.3 Evolution of Q as a Function of the Number of Turns N

Once the thickness is fixed, the maximum Q factor that one can achieve on a given footprint area S_{top} and form factor k is defined by the optimal number of turns N_{opt} . The optimal value is defined when

the derivative

$$\frac{dQ_a}{dN} = \frac{\beta}{\delta} \cdot \frac{-s_t \cdot N^2 - 2 \cdot s_t \cdot N + \sqrt{k \cdot S_{top}}}{\sqrt{k \cdot S_{top}} \cdot (N+1)^2}, \quad (17)$$

cancels. This is the case for

$$N_{opt} = \sqrt{\frac{\sqrt{k \cdot S_{top}} + s_t}{s_t}} - 1. \quad (18)$$

the evolution of Q as a function of the number of turn for given S_{top} , t , k is shown in the Figure 6. Three solenoids (B1, A3, B2) have been realized and characterized to validate experimentally the optimal number of turns. They are depicted in the Figure 7.

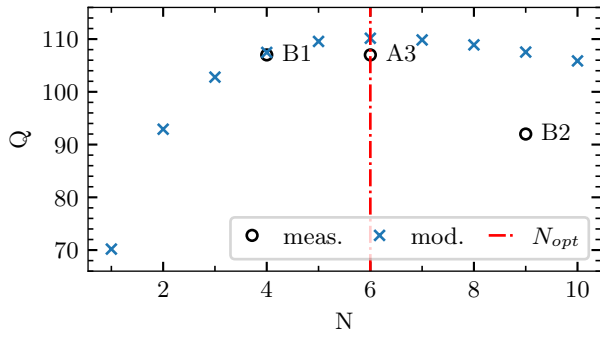


Fig. 6: Evolution of Q as a function of N for fixed thickness $t = 2$ mm, surface $S_{top} = 5.76$ cm², form factor $k = 1$ and frequency $f = 27.12$ MHz.

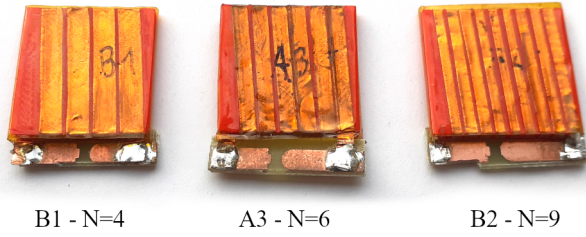


Fig. 7: Photograph of the solenoids B1, A3 and B2 characterized in Figure 6, with $l = 2.4$ cm, $w = 2.4$ cm, $t = 2$ mm, $s_t = 0.5$ mm.

For this specific case the optimal number of turns is 6. Around this value the evolution of Q is flat which can explain why the measurements do not show clearly the optimal number of turns. The discrepancy between point B2 and model value (roughly 20%) might be due to the irregularities on the width w_t of the copper tape cut by hand. Indeed, in this case, a 20% error on the width of the tape (2 mm) is equal to 400 μ m.

3.4 Optimal Q on a Given Footprint Area S_{top} and Thickness t

According to the previous results there is an optimal Q for given surface and thickness. This optimal Q is approximated by injecting Eq. (18) in Eq. (10) such that

$$Q_{a,opt} = \frac{\beta}{\delta} \cdot \frac{1}{\sqrt{k \cdot S_{top}}} \cdot \left(\sqrt{k \cdot S_{top}} + 2 \cdot s_t - 2 \cdot \sqrt{s_t \cdot (\sqrt{k \cdot S_{top}} + s_t)} \right). \quad (19)$$

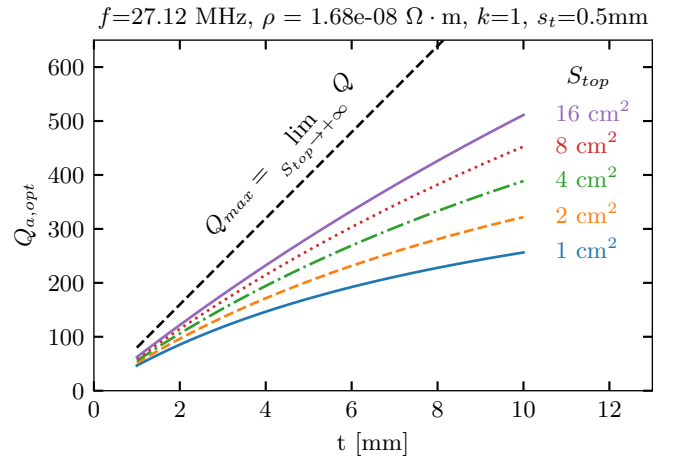


Fig. 8: Evolution of $Q_{a,opt}$ as a function of the thickness t and the footprint area S_{top} .

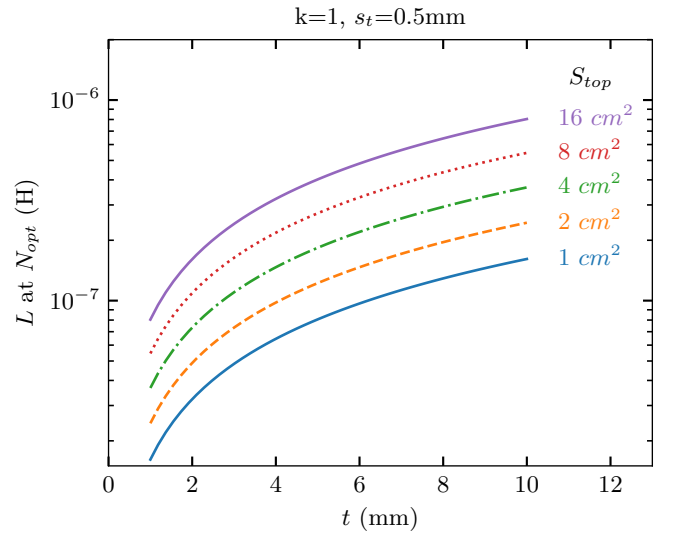


Fig. 9: Evolution of the inductance at N_{opt} as a function of the thickness t and the top surface S_{top} .

The evolution of $Q_{a,opt}$ as a function of the thickness t and the top surface S_{top} is plotted in Figure 8. According to Equation (10), under the assumption

that s_t is small in comparison to $l = \sqrt{k \cdot S_{top}}$, the Q factor is greater for greater S_{top} and reaches Q_{max} when $S_{top} \rightarrow \infty$ as presented in the Figure 8. Then the corresponding inductance is computed and plotted in the Figure 9. These two figures show that the Q factor of planar solenoids reaches limit ($Q \approx 200$) for a size compatible with Printed Circuit Board (PCB) process. It shows also that the achievable range of inductance with good quality factor is quite short, roughly 10 nH to 2 μ H.

4 Solenoids Tested Inside a VHF Converter

The converter under test is a $\Phi E2$ previously designed in [11]. The circuit diagram of the converter is presented in the Figure 10. The converter is made out of an inverter and a rectifier linked by a resonant series tank $L_s - C_s$. The inverter achieves naturally Zero Voltage Switching (ZVS) when sized properly [12]. The low voltage stress on the transistor is ensured thanks to the $L_{MR} - C_{MR}$ branch which resonates at two times the fundamental frequency of the converter. This filtering of the second harmonic ensures a maximum voltage of $2 \cdot V_{IN}$ on the transistor. The converter has been initially

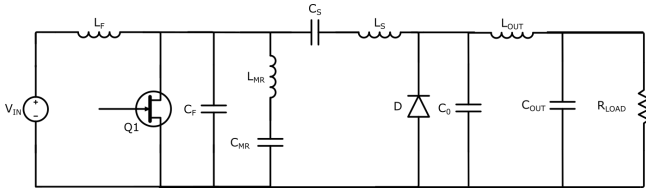


Fig. 10: Circuit diagram of the VHF converter.

designed with inductors made out of magnetic material (iron powder *Micrometal Mix-2*) as presented in Figure 11 a. Two inductors (L_{MR} and L_s) have been replaced by air core solenoids to show the performance and the limits of the air core technology. The air core solenoids have been designed with the following parameters and constraints: the thickness is fixed at $t = 5$ mm, the length l is fixed by the available space on the existing layout. Then the width w and the number of turns N are chosen to obtain the desired inductance value with Eq. (5) while keeping a reasonable volume and a small R_{AC} . The designed solenoids are sub-optimized because of the existing constraint on the length. The measured inductance and Q values are shown in the Table 2. The L_{MR} inductance has been measured at 27.12 MHz because the MR branch resonates at the second harmonic. This air core

Tab. 2: Measured inductance L and Q factor of the inductors L_{MR} and L_s .

Inductor	f (MHz)	L (nH)		Q factor	
		core	air	core	air
L_{MR}	27.12	217	206	167	122
L_s	13.56	420	325	265	122

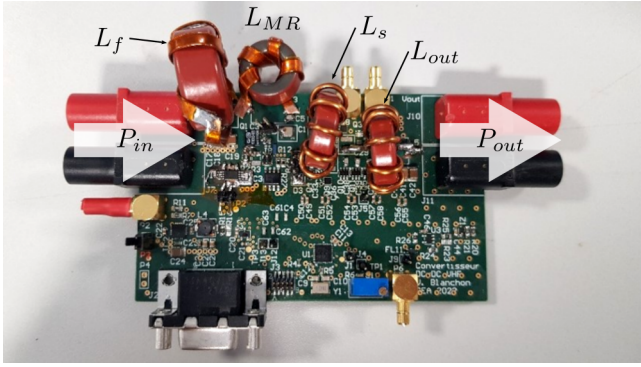
inductor shows similar performances to the core one with a relative difference on the inductance value of -5% and relative difference on Q value of -27% . The L_s inductor on the other hand works at the fundamental frequency 13.56 MHz and shows a relative difference on the inductance value of -22% and relative difference of Q value of -54% . The L_s case shows that it is harder to get a high Q with a lower frequency as expected by looking at Eq. (15). And at the same time the model for the inductance value is not accurate for solenoids with a greater width than length. This might be due to non uniformity of the magnetic field as already studied and well known on circular cross-section tape solenoids [13]–[15]. The adaptation of the formula to rectangular cross-section solenoids will be addressed in future work.

This drop of Q factor is mirrored on the global efficiency of the converter as shown in the table 3. The drop is due partly to a higher resistance value of the air core solenoid in comparison to the ring core with magnetic material and partly to the lower value of the inductance which causes the loss of the ZVS as depicted in the Figure 12 (higher magnitude oscillation around 0 in the case air).

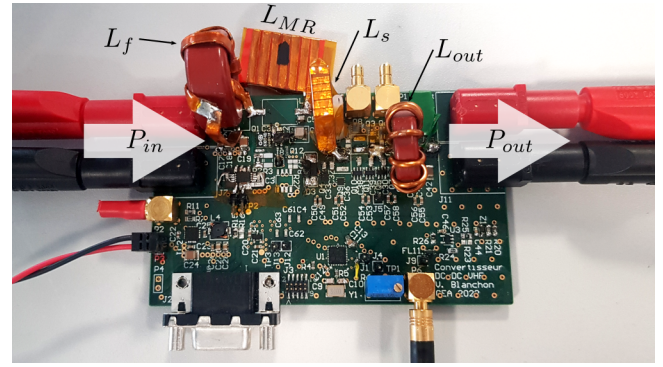
Tab. 3: Measured efficiency of the converter with standard powder core components and air core solenoids.

Case	P_{in} (W)	P_{out} (W)	η (%)
core	6.53	4.99	76.4
air	7.9	5.02	63.5

While the electrical performance is smaller with air core solenoids the mass power density is better as described in the Table 4. The L_{MR} component is 3 times lighter than the powder core one. At the same time the overall volume is 1.72 smaller when considering the powder core without the winding (3.77 cm^3) and 2.37 smaller when considering the overall volume (powder core and winding, $\approx 5.22 \text{ cm}^3$). The discrepancy of volume is due to



a.



b.

Fig. 11: Photographs of the converter with a. the ring core inductors and b. two air core solenoids.

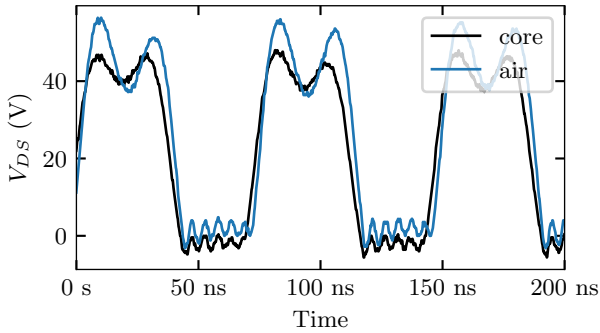


Fig. 12: Waveform of V_{DS} as a function of time.

the thickness and stiffness of the copper tape used for the powder core.

Tab. 4: Measured mass and volume of the inductance L_{MR} .

Case	Mass (g)	Core Volume (cm ³)
core	5.05	3.77
air	1.68	2.19

This comparison should be treated with caution, because the two types of components (the air core solenoids and the powder cores ones) have not been sized with exactly the same objectives and constraints due to the use of a pre-existing converter for the study case of one air core solenoids application. A more rigorous comparison will be applied in future study.

5 Conclusion

A simple analytical model has been checked against experiments and used to size two air core components for the replacement of standard powder core components. The design method is simple

and fast, and the characteristics of the components obtained correspond to those expected from the modeling for cases with small thickness and width in comparison to the length of the solenoid. Thanks to this model, it has been shown that the Q factor of air core solenoids made out of planar substrate is mainly constrained by the substrate thickness. In addition the asymptotic behavior of the Q factor with the footprint area tends to limit the achievable increase in performance within a reasonable area range.

In comparison to standard powder core component, the air core solenoids use less raw material (in term of mass) and have a larger volume.

This work shows the difficulty to exploit the advantages of air core technology (less material use) for VHF converter while keeping the electrical performances the same. One way to take advantage of the air core technology for VHF converters is to increase the resonant frequency to decrease the requirement in inductance and to improve at the same time the Q factor.

In the future, the model will be refined to take into account the drop of inductance for solenoids with a width greater than the length. The performance of the solenoid will be compared to other shapes like ring cores in terms of quality factor, radiated magnetic field and thermal performances.

6 Acknowledgment

This work is supported by the French National Research Agency in the framework of the "Investissements d'avenir" program (ANR-15-IDEX-02), via the project CDP PowerAlps.

References

- [1] J. Xu, Z. Tong, and J. Rivas-Davila, "1 kW MHz Wideband Class E Power Amplifier," *IEEE Open*

- Journal of Power Electronics*, vol. 3, pp. 84–92, 2022, Conference Name: IEEE Open Journal of Power Electronics. DOI: 10.1109/OJPEL.2022.3146835.
- [2] M. Madsen, A. Knott, and M. A. E. Andersen, “Low power very high frequency switch-mode power supply with 50 v input and 5 v output,” *IEEE Transactions on Power Electronics*, vol. 29, no. 12, pp. 6569–6580, 2014. DOI: 10.1109/TPEL.2014.2305738.
- [3] L. Pace, M. Beley, M. E. Khattabi, and A. Bréard, “Design and modeling of a 100w 1mhz gan-based single-switch resonant converter for high power density inherent pfc led driver,” in *2023 25th European Conference on Power Electronics and Applications (EPE'23 ECCE Europe)*, 2023, pp. 1–9. DOI: 10.23919/EPE23ECCEurope58414.2023.10264555.
- [4] L. Gu and J. Rivas-Davila, “1.7 kW 6.78 MHz Wireless Power Transfer with Air-Core Coils at 95.7% DC-DC Efficiency,” in *2021 IEEE Wireless Power Transfer Conference (WPTC)*, ISSN: 2573-7651, Jun. 2021, pp. 1–4. DOI: 10.1109/WPTC51349.2021.9458037.
- [5] M. Beley, M. El-Khattabi, L. Pace, and A. Bréard, “Analytical Design of a Finite Input Inductance 34.5 MHz Class E Inverter for Wireless Power Transfer,” in *International Conference on Integrated Power Electronics Systems*, Power Engineering Society VDE ETG, Düsseldorf, Germany, Mar. 2024.
- [6] M. Madsen, A. Knott, M. A. Andersen, and A. P. Mynster, “Printed circuit board embedded inductors for very high frequency Switch-Mode Power Supplies,” in *2013 IEEE ECCE Asia Downunder*, Jun. 2013, pp. 1071–1078. DOI: 10.1109/ECCE-Asia.2013.6579241.
- [7] J. D. Mønster, M. P. Madsen, J. A. Pedersen, and A. Knott, “Investigation, development and verification of printed circuit board embedded air-core solenoid transformers,” in *2015 IEEE Applied Power Electronics Conference and Exposition (APEC)*, ISSN: 1048-2334, Mar. 2015, pp. 133–139. DOI: 10.1109/APEC.2015.7104343.
- [8] M. Biglarbegian, N. Shah, I. Mazhari, and B. Parkhideh, “Design considerations for high power density/efficient PCB embedded inductor,” in *2015 IEEE 3rd Workshop on Wide Bandgap Power Devices and Applications (WiPDA)*, Nov. 2015, pp. 247–252. DOI: 10.1109/WiPDA.2015.7369285.
- [9] G. Zulauf, W. Liang, and J. Rivas-Davila, “A unified model for high-power, air-core toroidal PCB inductors,” in *2017 IEEE 18th Workshop on Control and Modeling for Power Electronics (COMPEL)*, Jul. 2017, pp. 1–8. DOI: 10.1109/COMPEL.2017.8013401.
- [10] Y. Wu and C. R. Sullivan, “Optimizations and Comparisons of Air-Core Inductors Based on a Semi-Analytical Calculation Toolkit,” in *2021 IEEE 22nd Workshop on Control and Modelling of Power Electronics (COMPEL)*, ISSN: 1093-5142, Nov. 2021, pp. 1–7. DOI: 10.1109/COMPEL52922.2021.9646075.
- [11] V. Blanchon, S. Carcouet, X. Maynard, and G. Despesse, “A 13.56MHz DC-DC Converter with Innovative Output Voltage Regulation,” in *13th International Conference on Power Electronics, Machines and Drives (PEMD 2024)*, Jun. 2024.
- [12] J. M. Rivas, O. Leitermann, Y. Han, and D. J. Perreault, “A Very High Frequency DC–DC Converter Based on a Class Φ_2 Resonant Inverter,” *IEEE Transactions on Power Electronics*, vol. 26, no. 10, pp. 2980–2992, 2011. DOI: 10.1109/TPEL.2011.2108669.
- [13] L. Lorenz, “Ueber die Fortpflanzung der Electricität,” en, *Annalen der Physik*, vol. 243, no. 6, pp. 161–193, 1879. DOI: 10.1002/andp.18792430602.
- [14] E. B. Rosa and F. W. Grover. “Formulas and Tables for the Calculation of Mutual and Self-inductance.” en. (1948), [Online]. Available: https://nvlpubs.nist.gov/nistpubs/bulletin/08/nbsbulletinv8n1p1_A2b.pdf.
- [15] D. W. Knight. “Solenoid Inductance Calculation.” (Feb. 2016), [Online]. Available: https://g3ynh.info/zdocs/magnetics/part_1.html (visited on 04/02/2024).